Current Science
CS 5 (3), 2391-2405 (2025)
Received 19 Feb 2025 | **Revised 14 March** 2025 | **Accepted 16 April**. 2025 | **Online Available 17 May** 2025
https://doi.org/ 10.52845/CS/2025-5-3-27

Current Science

Current Science

OPEN ACCESS

ISSN (O) 2795-8639

Original Article

AGTRAP: A Novel Prognostic Biomarker of Alternative Splicing Combined with Immune Cell Infiltration in Head and Neck Squamous Cell Carcinoma

Xingyue Xue[1#], Kun Cao[2#], Fang Lu[2], Qiang Bao[2], Jiafeng Li[2]*

[1]School of Stomatology, Xuzhou Medical University, Xuzhou 221004, China

[2]Department of Stomatology, Affiliated Hospital of Xuzhou Medical University, Xuzhou 221006, China

#These Authors Contributed Equally To This Study

***Corresponding Author: Jiafeng Li**

Abstract:

Objective: To construct a variable splicing prognostic model and explore the potential of key genes as prognostic biomarkers in head and neck squamous cell carcinoma (HNSC).

Methods: Download the RNA-Seq data of the HNSC cohort and the corresponding clinical data from the TCGA database, and download the alternative splicing data of HNSC from the TCGA SpliceSeq database. Identify the alternatively spliced events with differential expression according to the percent spliced in (PSI) values. Analyze the alternative splicing events related to prognosis and establish a prognostic risk model. Analyze the correlation between the model and prognosis and screen out the key genes. Combine with the analysis of immune cell infiltration to explore the prognostic impact of key genes on HNSC. Finally, the expression differences of the target genes in the tissues were verified by reverse transcription quantitative polymerase chain reaction (RT-qPCR).

Results: The AGTRAP gene was significantly highly expressed in the HNSC cohort. The occurrence frequency of the 670th alternative receptor site of AGTRAP increased in HNSC, and the overall expression level of the AGTRAP gene could serve as an independent prognostic risk indicator for HNSC.

Conclusions: The overall expression level of the AGTRAP gene can serve as a prognostic biomarker associated with alternative splicing combined with immune infiltration in HNSC.

Key words: **Head and neck squamous cell carcinoma; Alternative splicing; Tumor microenvironment; Immune cell infiltration; Prognosis**

Introduction

Head and neck squamous cell carcinoma (HNSC) is the most common malignant tumor in the head and neck region. Although there are some precancerous lesions manifested as leukoplakia or erythroplakia, most patients do not have a clinical history of precancerous lesions and have already reached the advanced stage when they seek medical treatment. Currently, HNSC lacks sensitive screening indicators, which undoubtedly adds numerous difficulties to the early diagnosis of this disease. Therefore, discovering biomarkers with excellent diagnostic potential is of great significance that cannot be ignored for the improvement of the clinical prognosis of HNSC patients.

Alternative splicing (AS), also known as selective splicing, refers to the process in which precursor messenger RNA undergoes different splicing patterns such as exon skipping and intron retention to generate multiple mature mRNA transcripts and translate them into different protein isoforms[1]. AS increases the complexity of the proteome, enabling a limited number of genes to encode more proteins to meet the complex functional requirements of organisms. It can also finely regulate gene expression at the post-transcriptional level and provide genetic

diversity for biological evolution. Abnormal alternative splicing is closely associated with the occurrence and development of various diseases, including tumors[2], neurodegenerative diseases[3], and so on. Abnormal alternative spliceosomes can serve as novel therapeutic targets for tumors[4].

The angiotensin II receptor-associated protein AGTRAP can inhibit the activation of angiotensin II and has been extensively studied in the fields of cardiovascular and metabolic diseases[5-9]. In addition, studies have found that AGTRAP can promote the progression of hepatocellular carcinoma[10] and colon cancer[11], which indicates its great potential as a biomarker for tumor prognosis.

In this study, a prognosis model related to alternative splicing in HNSC was constructed through public databases, and the key gene AGTRAP was screened out. The study analyzed the relationship between AGTRAP and the clinical characteristics as well as immune infiltration of HNSC, and preliminarily explored the potential functions of AGTRAP as a prognostic biomarker for HNSC.

2. Materials and Methods

2.1 Data and Sample Collection

The gene expression RNA-Seq data and clinical data were obtained from the The Cancer Genome Atlas (TCGA) database (https://portal.gdc.cancer.gov/), that is, the TCGA-HNSC dataset. The types of alternative splicing and the percent spliced in (PSI) values were obtained from the TCGA SpliceSeq database (https://bioinformatics.mdanderson.org/TCGASpliceSeq/).

Twenty pairs of HNSC tissues and adjacent normal tissues were collected from the Affiliated Hospital of Xuzhou Medical University and included in this study. The inclusion criteria were as follows: (1) Confirmed by histopathological examination; (2) No surgical treatment, radiotherapy or chemotherapy received before the operation; (3) Not suffering from other malignant tumors simultaneously. This study was approved by the Ethics Committee of the Affiliated Hospital of Xuzhou Medical University (Approval No.: XYFY2024-KL584-01), and all patients signed the informed consent forms.

2.2 Model Construction

Merge the alternative splicing data with the TCGA-HNSC data. Use univariate COX regression analysis to analyze the alternative splicing related to prognosis. With a filtering condition of $P < 0.05$, retain the significantly relevant alternative splicing results, draw an upset plot, and visualize the results through a volcano plot and a bubble plot. Use the "survival" package and the "glmnet" package to construct a survival model. Then, through LASSO regression and cross-validation, eliminate the AS with high correlation to construct the survival model. Calculate the risk scores according to the equation, and divide the samples into high-risk and low-risk groups based on the median value of the risk scores.

2.3 Survival Analysis

Use the "survival" package and the "survminer" package to conduct survival analysis on the high-risk and low-risk groups, and draw survival curves. Arrange all samples in ascending order according to the risk scores. Use the "pheatmap" package to draw scatter plots of survival status, risk curves, and heatmaps to observe the relationship between the risk scores and the survival status.

2.4 Model Validation

The "survival" package was used to conduct univariate and multivariate independent prognostic analyses on the model and other clinical traits to verify whether the model could serve as an independent prognostic factor independent of other clinical traits. The "survival", "survminer", and "timeROC" packages were employed to plot the receiver operating characteristic (ROC) curves of the model and other clinical traits respectively. The "rms" package was utilized to establish a risk - score - related nomogram incorporating clinical traits and generate a calibration curve.

2.5 Correlation Analysis between Alternative Splicing and Splicing Factors

Use the "limma" package to explore the correlation between prognosis - related AS and splicing factors. Set the filtering conditions as a correlation coefficient $r > 0.6$ and $P < 0.001$. Use Cytoscape software to visualize the regulatory network between alternative splicing and splicing factors。

2.6 Screening of Key Genes

Use the "limma", "ggplot2", and "ggpubr" packages to analyze the alternative splicing genes involved in constructing the prognostic model. Screen for genes with differential expression between tumor and normal tissues, setting the filtering criteria as |log2 *FC*| > 1 (*FC* represents the fold change) and $P < 0.05$, and visualize the results through box plots. Employ the "survival" and "survminer" packages to conduct survival analysis on the target genes. Divide them into high - and low - expression groups based on the expression levels, compare the survival differences between the two groups, and plot survival curves.

2.7 Clinical Correlation Analysis

Use the "limma" and "ggpubr" packages to perform a differential analysis on the expression levels of the target genes among different clinical subgroups and visualize the results.

2.8 Immune Cell Infiltration Analysis

Use the "limma", "ggplot2", and "ggpubr" packages to conduct a differential analysis of immune checkpoint - related genes in the high - and low - expression groups. To further observe the potential differences in immune cell infiltration between the high - and low - expression groups, use the "CIBERSORT" package to calculate the proportions of immune cell subsets in these two groups. Employ the "GSVA" and "GSEABase" packages to compare the differences in immune - related functions between the high - and low - expression groups. Analyze the correlation between the expression level of the target gene and immune cells, and use the "ggplot2" package to visualize the results.

2.9 Enrichment Analysis

The STRING database (https://cn.string-db.org/) was used to construct a protein - protein interaction network, and the top 200 genes were extracted. The "clusterProfiler", "org.Hs.eg.db", "enrichplot", "ggplot2", "circlize", "RColorBrewer", "dplyr", and "ComplexHeatmap" packages were employed to conduct KEGG enrichment analysis on these genes.

2.10 Tissue Verification

The total RNA was extracted using the RNApure Tissue & Cell Kit (DNase I). Then, cDNA was synthesized with the PrimeScript™ RT Master Mix (TAKARA) kit. Fluorescent quantitative PCR was carried out using the SYBR Green Pro Taq HS Premixed qPCR kit. The primer sequences were designed as follows: Forward primer (F): 5'- GATGCCCGAGGGTACTGAAG -3'; Reverse primer (R): 5'- TCCCTAGAACGACCTCCCAG -3'.

2.11 Data Analysis

All statistical analyses and plotting were performed using R software version 4.3.3. The regulatory network between alternative splicing and splicing factors was visualized using Cytoscape software. A *P* - value less than 0.05 was considered statistically significant.

3. Reuslts

3.1 Data Collection

A total of 527 cases of TCGA - HNSC with complete gene expression and clinical data were obtained from the TCGA database. The alternative splicing types and PSI values of HNSC were acquired from the TCGA SpliceSeq database. The alternative splicing data were merged with the TCGA - HNSC dataset. Univariate COX regression analysis was used to identify the alternative splicing events related to prognosis. Upset plots were drawn, and the results were visualized through volcano plots and bubble plots. See Figure 1. As can be seen from the figure, among the alternative splicing events related to HNSC prognosis, exon skipping (ES) had the highest occurrence frequency, while mutually exclusive exons (ME) had the lowest. Taking the alternative acceptor site (AA) as an example, AGTRAP|670|AA had the lowest *P* - value, indicating that this alternative splicing event was most likely to be associated with prognosis.

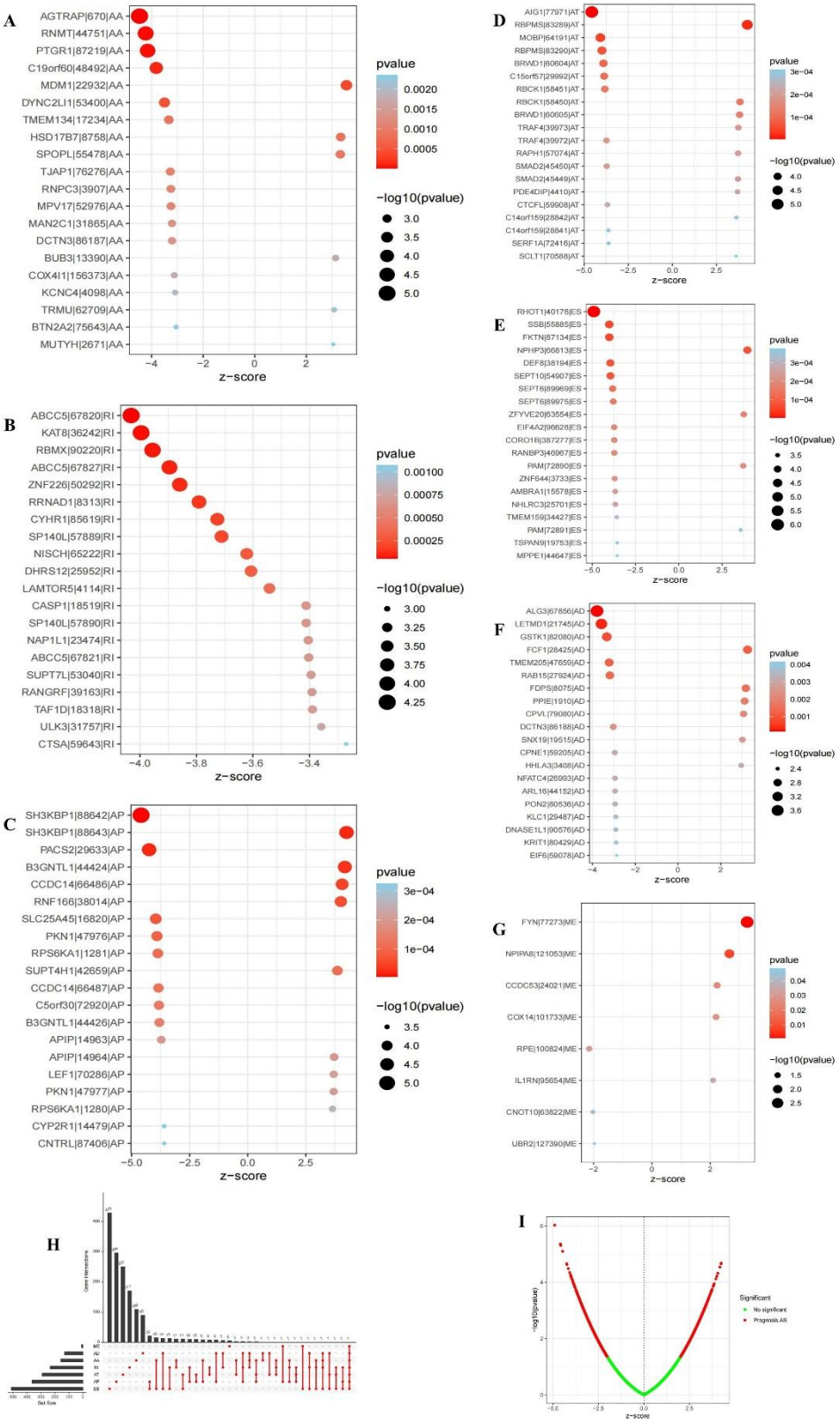

Figure 1 Alternative splicing related to prognosis in HNSC.
A: Alternate acceptor site (AA). B: Retained intron (RI). C: Alternate promoter (AP). D: Alternate terminato (AT). E: Exon skip (ET). F: Alternate Donor site (AD). G: Mutually exclusive exons (ME). H： UniCoxUpset of AS in HNSC. I: prognosis AS.

3.2 Model Construction

Highly correlated AS events were screened out through LASSO regression and cross - validation to prevent model overfitting. See Figure 2. Finally, the most optimal 12 prognosis - related

AS events were selected to construct the survival model. The model formula is as follows: Risk score = PSI1×coef1 + PSI2×coef2 + …… + PSIn×coefn (where coef represents the gene risk coefficient). See Table 1.

Tab. 1 Genes involved in the survival model and their risk coefficients

ID	coef
RHOT1|40176|ES	-2.371
SH3KBP1|88642|AP	-1.183
AGTRAP|670|AA	-1.478
SH3KBP1|88643|AP	0.526
PACS2|29633|AP	-1.978
B3GNTL1|44424|AP	0.759
MOBP|64191|AT	-1.136
ABCC5|67820|RI	-1.090
FKTN|87134|ES	-2.312
RBPMS|83290|AT	-2.391
NPHP3|66813|ES	0.724
SLC25A45|16820|AP	-1.783

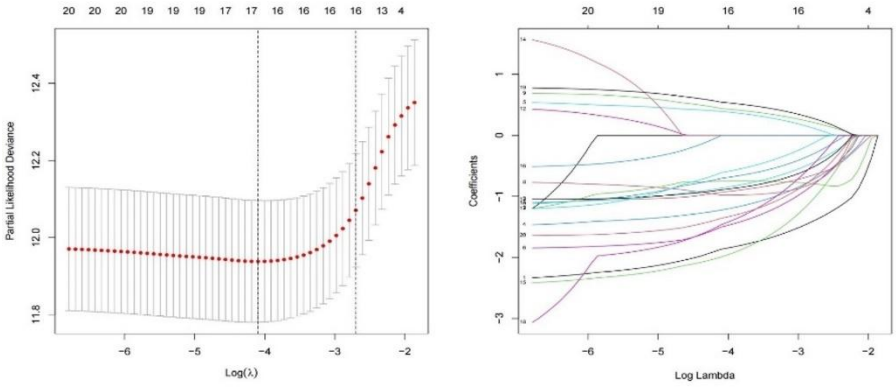

Figure 1 LASSO regression and cross-validation.

3.3 Survival Analysis

Calculate the risk score according to the equation, and divide the samples into high-risk and low-risk groups based on the median value of the risk score. Perform survival analysis on the high-risk and low-risk groups to explore the relationship between the risk score and the survival status. Arrange all the samples in ascending order according to the risk score, and observe the survival status of each sample. See Figure 3. As time goes by, the survival rate of the high-risk group is lower than that of the low-risk group, and there is a significant difference in the survival status between the high-risk and low-risk groups. In addition, as the risk score increases, the number of deaths also increases accordingly. From the risk heat map, it can be seen that as the risk score increases, the PSI value of AGTRAP|670|AA gradually decreases, which means a low-risk alternative splicing. In contrast, SH3KBP1|88643|AP is a high-risk alternative splicing.

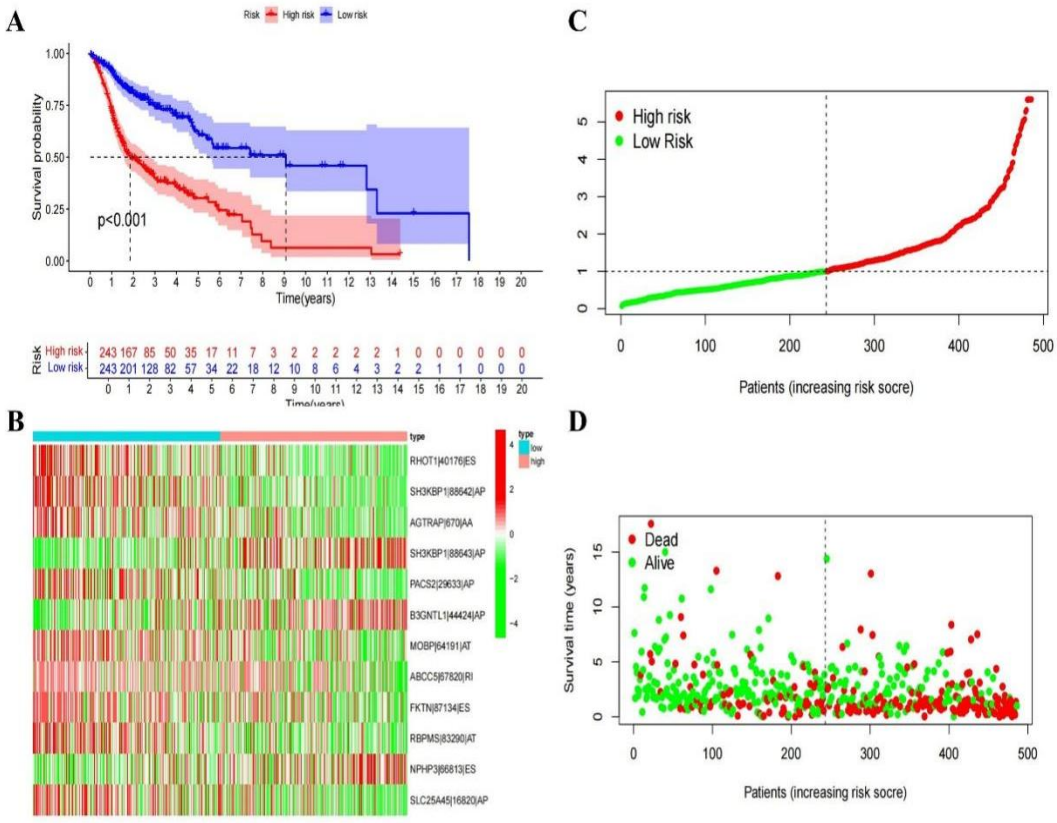

Figure 2 Survival curve, scatter plot of survival status and risk heat map.

A: The survival differences between the high-risk group and the low-risk group. B: The change of the expression level of AS with the risk score. C-D: The change of survival status with the risk score.

3.4 Model Validation

Through univariate and multivariate independent prognostic analyses, it was verified that the model could serve as an independent prognostic factor for Head and Neck Squamous Cell Carcinoma (HNSC) independently of other clinical traits. As can be seen from the Receiver Operating Characteristic (ROC) curve, in the constructed model, the areas under the curve for 1 year, 2 years, and 3 years are all higher than 0.7. This demonstrates that the model has a high sensitivity in predicting the survival rate of HNSC, and the prediction probability of the model is superior to other clinical traits. See Figure 4.

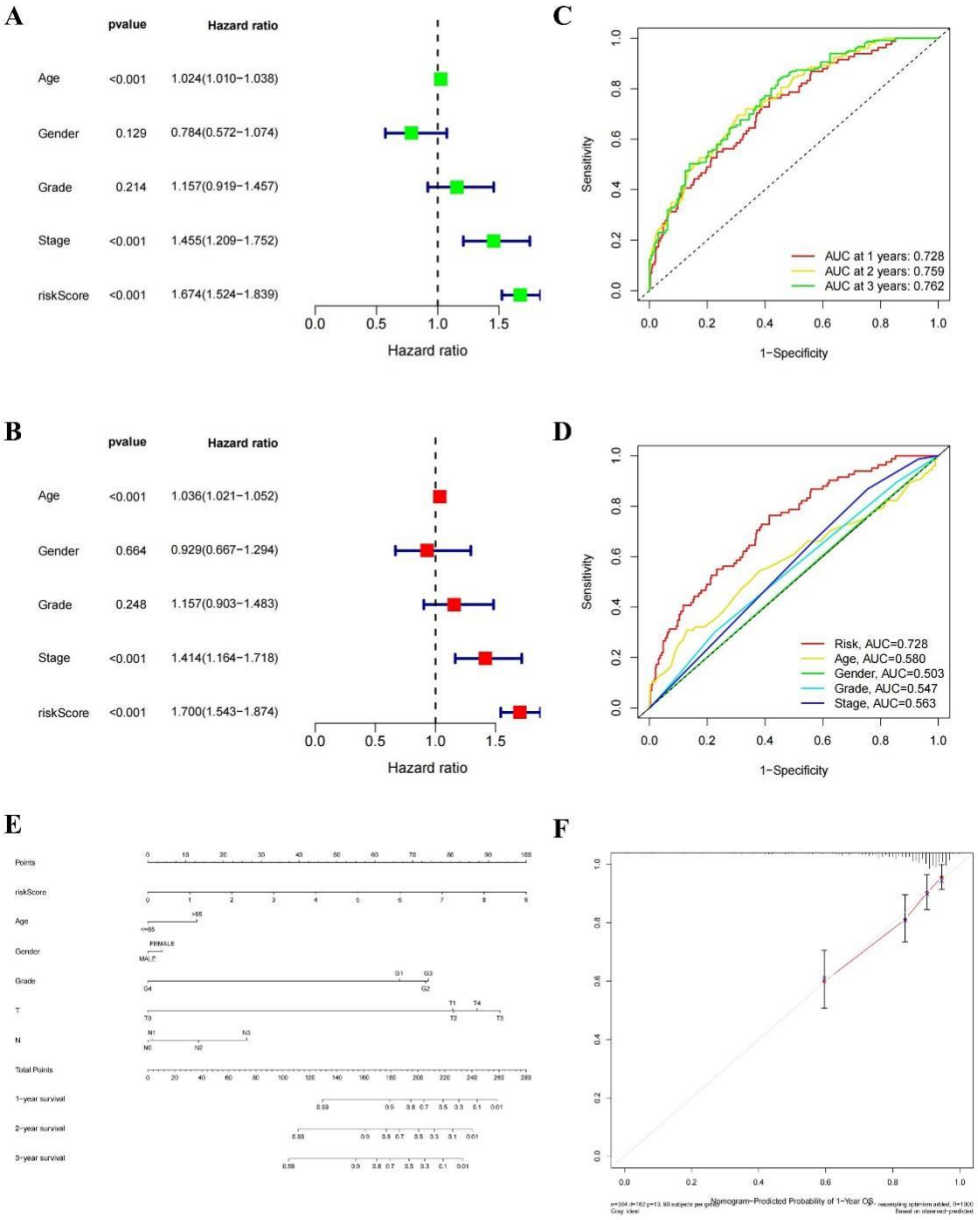

Figure 3 Construction and validation of model

A: Univariate Cox regression analysis. B: Multivariate Cox regression analysis.C-D: The ROC curves of the model and other clinical traits. E: Nomogram. F: Calibration curve.

3.5 Correlation Analysis between Alternative Splicing and Splicing Factors

In order to explore the correlation between prognosis-related alternative splicing (AS) and splicing factors, the Cytoscape software was used to visualize the regulatory network of alternative splicing and splicing factors. See Figure 5.

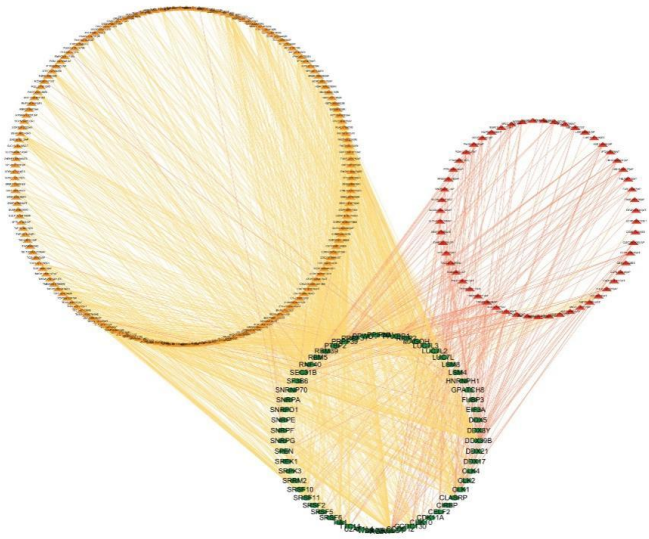

Figure 5 The regulatory network of AS and splicing factors

3.6 Gene Differential Analysis

A differential analysis of the expression levels of alternative splicing genes involved in the construction of the prognostic model was carried out. It was found that the average expression level of the gene AGTRAP in tumor tissues was 5.021, which was higher than the average expression level of 3.783 in normal tissues. $\log_2 FC$ =1.238, P=1.491e-17. Subsequently, the samples were divided into high-expression and low-expression groups according to the expression level of AGTRAP, and survival analysis was performed on the two groups. As can be seen from the survival curve, there was a significant survival difference between the high-expression and low-expression groups (P < 0.001), indicating that the gene AGTRAP was associated with the prognosis of Head and Neck Squamous Cell Carcinoma (HNSC). Moreover, when the expression level was lower than the threshold value of 4.750, the prognosis of the low-risk group was better than that of the high-risk group. However, when it was higher than the threshold value, the prognosis of the high-risk group became better than that of the low-risk group. See Figure 6.

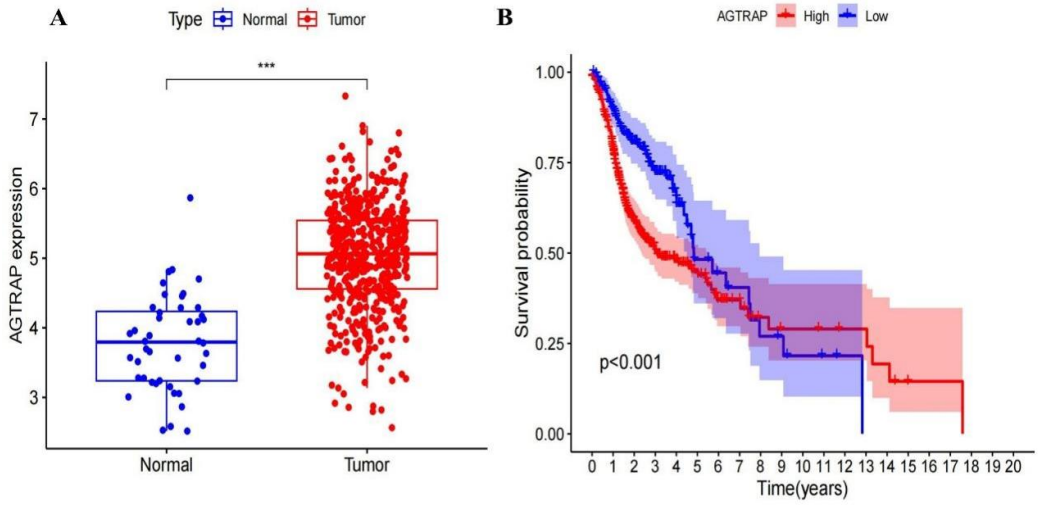

Figure 6 Analysis of the expression levels of AGTRAP and survival differences. A: Differencet expression levels between cancer and adjacent normal tissues. B: Analysis of survival differences between high - and low - expression groups. *** P＜0.001.

3.7 Clinical Correlation Analysis

In order to explore whether the expression level of AGTRAP can distinguish different clinical stages, a differential analysis of the gene expression levels among different clinical trait groups was

conducted. The number of samples with distant metastasis, i.e., M1, was too small (n = 1), so they did not participate in this clinical group comparison. As can be seen from the box plot, there was a difference in the expression level of AGTRAP between T1 and T4, and the expression level in the G4 group was lower than that in the other grades. There was no obvious difference among the other clinical groups. See Figure 7.

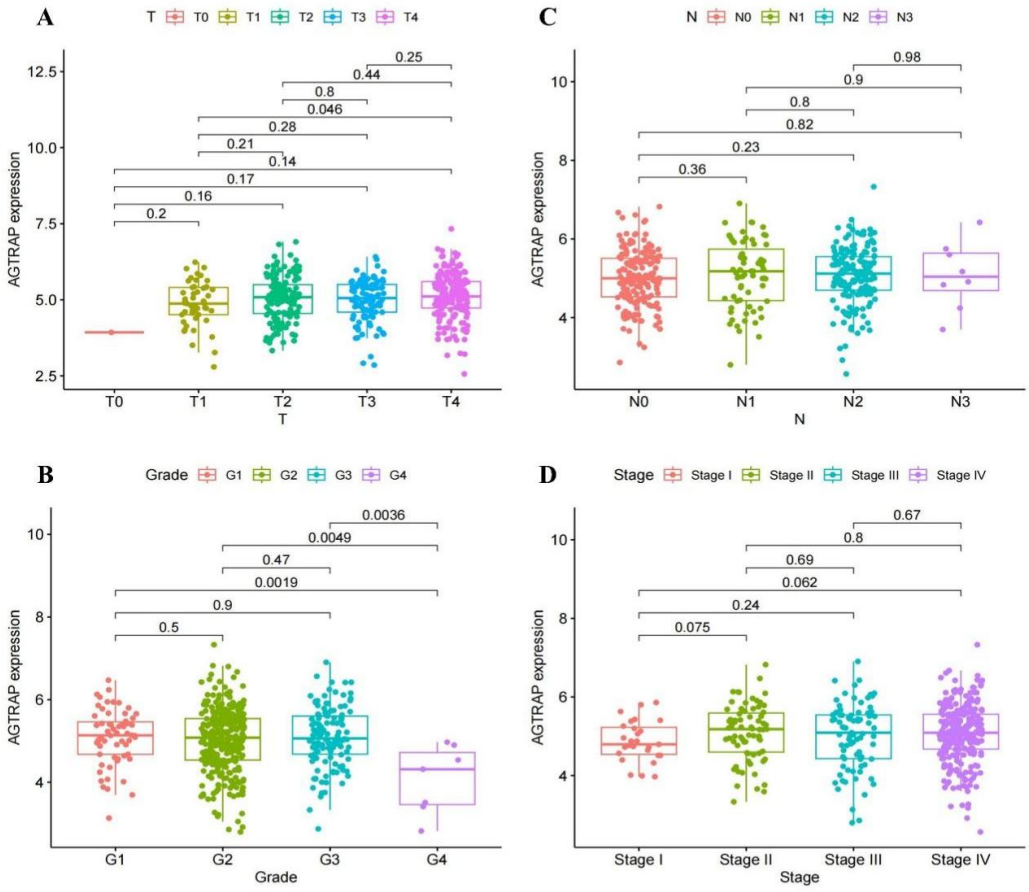

Figure 7 Analysis of clinical relevance.
A: Differences in gene expression among different T – groups. B: Differences in gene expression among different N – groups. C: Differences in gene expression among different grade– groups. D: Differences in gene expression among different stage – groups.

3.8 Immune Correlation Analysis

In order to further observe the potential differences in immune cell infiltration between the high-expression and low-expression groups, the proportions of immune cell subsets in the high-expression and low-expression groups were calculated, the differences in immune-related functions and immune checkpoint-related genes between the high-expression and low-expression groups were compared, and the correlation between the expression level of AGTRAP and immune cells was analyzed. As can be seen from the box plot and scatter plot, the proportions of naive B cells and plasma cells in the high-expression group were lower than those in the low-expression group, and they were negatively correlated with the gene expression level. The proportion of activated natural killer (NK) cells in the high-expression group was higher than that in the low-expression group, and it was positively correlated with the gene expression level. The immune scores of the high-expression group in terms of para-inflammation, T helper 1 (TH1) cells, and type I interferon response were higher than those of the low-expression group, while in terms of B cells, major histocompatibility complex class I, and type II interferon response, the immune scores of the low-expression group were higher. The expression levels of immune checkpoint-related genes such as CD276 and TNFRSF14 in the high-expression group were higher than those in the low-expression group,

while in immune checkpoints such as CD27, TNFSF15, CTLA-4, and CD200, the expression levels in the low-expression group were higher. See Figure 8.

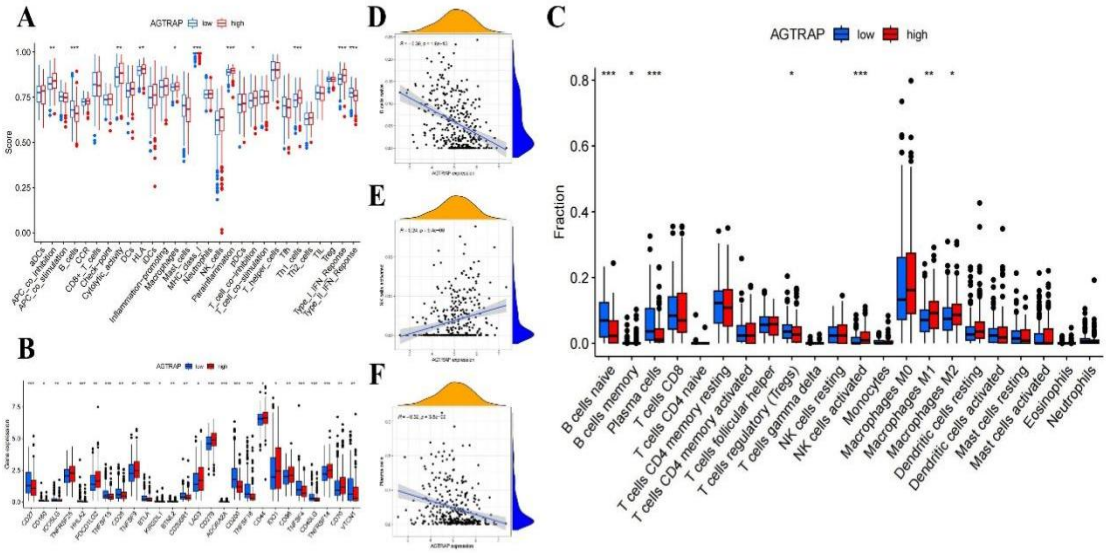

Figure 8 Immune infiltration analysis

A、C: Differences in immune cells and immune functions. B: Differences in checkpoint. D: The relationship between naive B cells and gene expressio. E: The relationship between activated NK cells and gene expression. F: The relationship between plasma cells and gene expression. * *P*＜0.05. ** *P*＜0.01. * *P*＜0.001.**

3.9 Enrichment Analysis

The top 10 genes related to AGTRAP were identified through the STRING database, namely CLCN6, CAMLG, BDKRB2, AGT, CHRM3, AGTR1, RACK1, ARAP1, PITPNG, and BDKRB1. A protein-protein interaction network was drawn. In order to further explore the molecular mechanism of AGTRAP, the top 200 genes were extracted and a Kyoto Encyclopedia of Genes and Genomes (KEGG) analysis was performed on them. The results showed that the biological functions of AGTRAP mainly focused on "neuroactive ligand-receptor interaction", "hormone signaling pathway", "calcium signaling pathway", "cholinergic synapse", "relaxin signaling pathway", "PI3K-Akt signaling pathway", "chemokine signaling pathway", and "chemokine signaling pathway". See Figure 9.

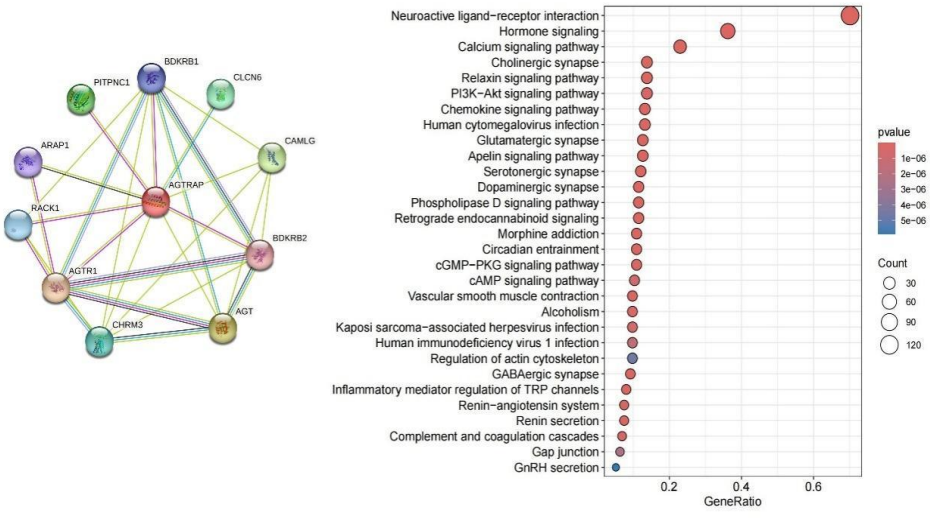

Figure 9 PPI and KEGG analysis

3.10 Tissue Verification

The difference in the expression level of AGTRAP was verified in 20 pairs of Head and Neck Squamous Cell Carcinoma (HNSC) tissues and adjacent normal tissues. The results of Reverse Transcription Quantitative Polymerase Chain Reaction (RT-qPCR) showed that, compared with the adjacent normal tissues, the expression level of AGTRAP in the cancer tissues was significantly increased, which was consistent with the previous bioinformatics analysis results. See Figure 10.

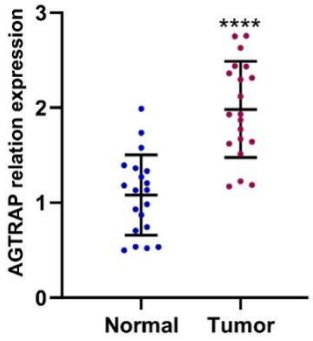

Figure 10 The results of the RT-qPCR experiment
****** *P* < 0.0001.**

4. Discussion

The global incidence of head and neck squamous cell carcinoma (HNSC) ranks sixth among malignant tumors. Smoking, excessive alcohol consumption, and high-risk human papillomavirus (HPV) infection are its main risk factors[12]. In the early stage, the symptoms of HNSC are insidious, and there is a lack of characteristic screening indicators, resulting in a 5-year survival rate of HNSC of less than 70%[13].

Abnormal splicing events can act as oncogenic drivers and/or bystander factors leading to tumor progression[14]. There are significant differences in the expression levels or splicing patterns of these events in tumor tissues compared with normal tissues. Chitra Rawat and Hannelore V Heemers revealed that alternative splicing events result in treatment resistance and the emergence of new phenotypes in prostate cancer[15]. Yen K Lieu and others discovered that abnormal splicing of MAP3K7 induced by SF3B1 mutants leads to anemia in myelodysplastic syndromes[16]. Ma and others[17] found through their research that RALYL can coordinate the alternative splicing of MNK2 by binding to HNRNPC, potentially inhibiting the progression of colorectal cancer. Detecting abnormal splicing events is helpful for the early diagnosis of tumors and the monitoring of the disease condition.

In this study, through the TCGA and TCGA SpliceSeq databases, the clinical data, gene expression levels, alternative splicing types, and splicing percentages related to HNSC were integrated. A total of 2,302 alternative splicing events associated with the prognosis of HNSC were identified through univariate COX regression analysis. Subsequently, 12 alternative splicing events significantly related to the prognosis were screened out to construct a prognostic risk model. The model was integrated with gender, age, clinical grade, tumor size, and lymph node metastasis status to create a nomogram for the combined prediction of patients' prognosis. The predictive value of the model was verified through survival analysis and independent prognostic analysis, and the area under the ROC curve also showed good sensitivity and specificity.

AGTRAP is a regulatory protein that interacts with the type I angiotensin II receptor and is capable of negatively regulating the angiotensin II signaling pathway[18]. Pan-cancer analysis has demonstrated that the high expression of AGTRAP is correlated with poor prognosis in diverse cancers[19]. Through constructing a gene co-expression network, Zeng[20] identified that AGTRAP is highly expressed in tongue squamous cell carcinoma and is linked to a poor prognosis. However, the research conducted by Claudia Alexandra Dumitru and others[21] indicated that

AGTRAP also shows a high expression level in glioblastoma and is associated with an unfavorable prognosis. Saioa Mendaza[22] discovered that cytoplasmic p16 interacts with AGTRAP and is overexpressed in cervical cancer. In line with various studies, during our research on head and neck squamous cell carcinoma, we observed that AGTRAP is expressed at a high level. Moreover, when the expression level of this gene exceeds the threshold of 4.750, it is associated with a poor prognosis.

In order to explore more comprehensively whether there are differences in AGTRAP at different stages of HSNC, we grouped and analyzed various clinical traits. Given that the sample size of patients with distant metastasis was extremely small (n = 1), they were not included in the analysis. The findings revealed that there was a difference in the expression level of AGTRAP between T1 and T4, and the expression level in the G4 group (n = 7) was lower compared to that in the other grades. Additionally, there were no significant statistical differences in terms of different tumor sizes, lymph node metastases, tumor grades, and tumor stages. We hypothesize that the expression level of AGTRAP is not associated with the aforementioned clinical parameters. In the study, in patients with a higher tumor grade, the level of AGTRAP in their bodies was correspondingly higher, and the survival prognosis was poorer[23]. Moreover, no obvious difference in AGTRAP was observed among different lymph node metastasis conditions. In the future, it will be necessary to increase the sample size to further investigate the relationship between the expression level of AGTRAP and the clinical progression of tumors.

Immune infiltration is an important determinant of cancer prognosis[24]. To evaluate the association between AGTRAP and immune infiltration, we analyzed the immune cells in the tumor microenvironment for the high and low expression groups, and also analyzed the immune-related functions and immune checkpoints. Activated natural killer (NK) cells and M1 macrophages were more abundant in the high expression group, while plasma cells and B cells, especially naive B cells, were more abundant in the low expression group. NK cells can recognize and eliminate tumor cells that have escaped the immune surveillance of $CD8^+$ T cells, playing a crucial role in the body's anti-tumor immune defense[25]. Chimeric antigen receptor-natural killer (CAR-NK) cells also show good potential in the treatment of HNSC[26, 27]. Previous studies have shown that M1 macrophages can inhibit tumor progression and have a pro-inflammatory effect[28]. This is consistent with the high immune score of the high expression group in parainflammation (PI). Sixty-five to 85% of HNSC cases have p53 mutations, which are associated with a poor prognosis[29]. It is known that PI acts in synergy with p53 to inhibit tumor progression. However, in the absence of p53, PI will instead promote the carcinogenic process[30]. Targeted inhibition of p53 mutations, exerting the anti-tumor effect of M1 macrophages and the synergistic effect between PI and p53, has potential therapeutic value for HNSC. Studies have shown that a high density of naïve B cells can enhance anti-tumor immunity in pancreatic ductal adenocarcinoma and non-small cell lung cancer, and is associated with a good prognosis[31, 32]. In addition, the combination of programmed cell death protein 1 (PD-1) inhibitors and Bcl6 blockade in the treatment of pancreatic cancer can promote the differentiation of naive B cells into plasma cells and increase the sensitivity to immune checkpoint inhibitors[33]. Except for CD44 and CD276, the expression levels of most immune checkpoints in the high expression group were lower than those in the low expression group. Compared with the low expression group, the expression level of genes related to the immune checkpoint cytotoxic T lymphocyte-associated protein 4 (CTLA-4) in the high expression group was significantly lower. Targeted inhibition of CTLA-4 can activate T cells, release interferon and tumor necrosis factor, up-regulate the body's anti-tumor immunity, and promote the apoptosis of tumor cells[34]. We speculate that the high expression group may achieve better efficacy than the low expression group with inhibitors such as CTLA-4. In conclusion, the grouping of AGTRAP may help distinguish the immune and molecular characteristics, screen treatment options, and predict the prognosis of HNSC.

From the KEGG analysis, it can be seen that AGTRAP and related genes are enriched in the PI3K/Akt/mTOR signaling pathway. Existing research results show that the PI3K/Akt/mTOR signaling is active in more than 90% of head and

neck cancers[35]. Ana Elizia Mascarenhas Marques[36] have also confirmed the increased expression of the PI3K/Akt/mMTOR pathway in HNSC. ATRAP can activate the PI3K/Akt/mTOR signaling pathway during cancer progression[37]. In addition, SU[38] and Jiang[39] have found that targeted regulation of the PI3K/Akt/mMTOR pathway can reduce the radiotherapy resistance of HNSC and improve the treatment effect. AGTRAP is expected to become a molecular targeted therapy target for the targeted regulation of the PI3K/Akt/mMTOR pathway in HNSC. Interestingly, according to the enrichment analysis, AGTRAP is associated with alcoholism. Excessive alcohol consumption is one of the main risk factors for HNSC[40]. In addition, excessive alcohol consumption can lead to microbial dysbiosis in HNSC, promoting carcinogenesis and metastasis[41]. The synergistic effect of AGTRAP and alcohol promotes the occurrence and development of HNSC, which is worthy of further research in the future.

Nevertheless, this study still has some limitations. Firstly, the bioinformatics analysis is based on the single TCGA database, and the histological experiments are verified with a small sample size from a single center. In the future, it would be possible to combine multiple databases and conduct multi-center analyses. Considering the expression differences of AGTRAP, it is still necessary to further explore the control threshold of AGTRAP in the future. Additionally, the mechanism by which AGTRAP affects HNSC remains to be further explored in the future.

In conclusion, we constructed a prognostic model of alternative splicing for head and neck squamous cell carcinoma (HNSC), and found that the key gene AGTRAP is highly expressed in HNSC and is associated with a poor prognosis. AGTRAP may affect HNSC through the PI3K/Akt/mTOR signaling pathway. The overall expression level of AGTRAP can serve as a prognostic biomarker related to alternative splicing combined with immune infiltration in HNSC.

Conflict of interest

The authors declare that they have no conflict of interest.

Funding sources

This research did not receive any specific grant from funding agencies in the public, commercial, or not-for-profit sectors.

References

1. marasco L E, Kornblihtt A R. The physiology of alternative splicing [J]. Nature reviews Mol ecular cell biology, 2023, 24(4).242-54.
2. Biamonti G, Catillo M, Pignataro D, et al. The alternative splicing side of cancer [J]. Seminar s in cell & developmental biology, 2014,3230-6.
3. Nikom D, Zheng S. Alternative splicing in neu rodegenerative disease and the promise of RN A therapies [J]. Nature reviews Neuroscience, 2023, 24(8).457-73.
4. BONNAL S, VIGEVANI L, Valcárcel J. The s pliceosome as a target of novel antitumour dru gs [J]. Nature reviews Drug discovery, 2012, 1 1(11).847-59.
5. Fujimoto D, Kuwabara T. Combination of AT RAP deletion and angiotensin II accelerates D KD progression, which may also accelerate D KD research [J]. Hypertension research : offici al journal of the Japanese Society of Hyperten sion, 2025, 48(3).1223-4.
6. Haruhara K, Suzuki T, Wakui H, et al. Deficie ncy of the kidney tubular angiotensin II type1 receptor-associated protein ATRAP exacerbate s streptozotocin-induced diabetic glomerular i njury via reducing protective macrophage pola rization [J]. Kidney international, 2022, 101 (5).912-28.
7. Lu Y, Zhang J, Han B, et al. Extracellular vesi cles DJ-1 derived from hypoxia-conditioned h MSCs alleviate cardiac hypertrophy by suppre ssing mitochondria dysfunction and preventin g ATRAP degradation [J]. Pharmacological res earch, 2023, 187106607.
8. Tamura K, Azushima K, Kinguchi S, et al. AT RAP, a receptor-interacting modulator of kidn ey physiology, as a novel player in blood press ure and beyond [J]. Hypertension research : of ficial journal of the Japanese Society of Hyper tension, 2022, 45(1).32-9.
9. Tsukamoto S, Suzuki T, Wakui H, et al. Angiot ensin II type 1 receptor-associated protein in i mmune cells: a possible key factor in the path ogenesis of visceral obesity [J]. Metabolism: c linical and experimental, 2023, 149155706.
10. Wang L, Zhang W, Yang T, et al. Construction and Comprehensive Analysis of a Stratificatio n System Based on AGTRAP in Patients with

Hepatocellular Carcinoma [J]. Disease markers, 2021, 20216144476.
11. Sanz-Pamplona R, Gil-Hoyos R, López-Doriga A, et al. Mutanome and expression of immune response genes in microsatellite stable colon cancer [J]. Oncotarget, 2016, 7(14).17711-25.
12. Johnson D E, Burtness B, Leemans C R, et al. Head and neck squamous cell carcinoma [J]. Nature reviews Disease primers, 2020,6(1).92.
13. Pulte D, Brenner H. Changes in survival in head and neck cancers in the late 20th and early 21st century: a period analysis [J]. The oncologist, 2010, 15(9).994-1001.
14. Zhang Y, Qian J, Gu C, et al. Alternative splicing and cancer: a systematic review [J]. Signal transduction and targeted therapy, 2021,6(1).78.
15. Rawat C, Heemers H V. Alternative splicing in prostate cancer progression and therapeutic resistance [J]. Oncogene, 2024, 43(22).1655-68.
16. Lieu Y K, Liu Z, Ali A M, et al. SF3B1 mutant-induced missplicing of MAP3K7 causes anemia in myelodysplastic syndromes [J]. Proceedings of the National Academy of Sciences of the United States of America, 2022, 119(1).
17. Ma Z, Zhu J, Chen M, et al. RALYL Overexpression Suppresses Colorectal Cancer via Modulating HNRNPC-Mediated MNK2 Alternative Splicing [J]. Cancer reports (Hoboken, NJ), 2025, 8(3).e70179.
18. Lopez-Ilasaca M, Liu X, Tamura K, et al. The angiotensin II type I receptor-associated protein, ATRAP, is a transmembrane protein and a modulator of angiotensin II signaling [J]. Molecular biology of the cell, 2003, 14(12).5038-50.
19. Hong K, Zhang Y, Yao L, et al. Pan-cancer analysis of the angiotensin II receptor-associated protein as a prognostic and immunological gene predicting immunotherapy responses in pan-cancer [J]. Frontiers in cell and developmental biology, 2022, 10913684.
20. Zeng H, Li H, Zhao Y, et al. Transcripto-based network analysis reveals a model of gene activation in tongue squamous cell carcinomas [J]. Head & neck, 2019, 41(12).4098-110.
21. Dumitru C A, Walter N, Siebert C L R, et al. The Roles of AGTRAP, ALKBH3, DIVERSIN, NEDD8 and RRM1 in Glioblastoma Pathophysiology and Prognosis [J]. Biomedicines, 2024, 12(4).
22. Mendaza S, Fernández-Irigoyen J, Santamaría E, et al. Absence of Nuclear p16 Is a Diagnostic and Independent Prognostic Biomarker in Squamous Cell Carcinoma of the Cervix [J]. International journal of molecular sciences, 2020, 21(6).
23. Liu S, Zhao W, Li X, et al. AGTRAP Is a Prognostic Biomarker Correlated With Immune Infiltration in Hepatocellular Carcinoma [J]. Front Oncol, 2021, 11713017.
24. Braun D A, Hou Y, Bakouny Z, et al. Interplay of somatic alterations and immune infiltration modulates response to PD-1 blockade in advanced clear cell renal cell carcinoma [J]. Nature medicine, 2020, 26(6).909-18.
25. Sivori S, Pende D, Quatrini L, et al. NK cells and ILCs in tumor immunotherapy [J]. Molecular aspects of medicine, 2021, 80100870.
26. Ciulean I S, Fischer J, Quaiser A, et al. CD44v6 specific CAR-NK cells for targeted immunotherapy of head and neck squamous cell carcinoma [J]. Front Immunol, 2023, 141290488.
27. Nowak J, Bentele M, Kutle I, et al. CAR-NK Cells Targeting HER1 (EGFR) Show Efficient Anti-Tumor Activity against Head and Neck Squamous Cell Carcinoma (HNSCC) [J]. Cancers, 2023, 15(12).
28. Cendrowicz E, Sas Z, BREMER E, et al. The Role of Macrophages in Cancer Development and Therapy [J]. Cancers, 2021, 13(8).
29. Li M, Sun D, Song N, et al. Mutant p53 in head and neck squamous cell carcinoma: Molecular mechanism of gain-of-function and targeting therapy (Review) [J]. Oncology reports, 2023, 50(3).
30. Aran D, Lasry A, Zinger A, et al. Widespread parainflammation in human cancer [J]. Genome biology, 2016, 17(1).145.
31. Chen J, Tan Y, Sun F, et al. Single-cell transcriptome and antigen-immunoglobin analysis reveals the diversity of B cells in non-small cell lung cancer [J]. Genome biology, 2020, 21(1).152.
32. Zhang S, Ta N, Zhang S, et al. Unraveling pancreatic ductal adenocarcinoma immune prognostic signature through a naive B cell gene set [J]. Cancer letters, 2024, 594216981.
33. Mirlekar B, Wang Y, Li S, et al. Balance between immunoregulatory B cells and plasma cells drives pancreatic tumor immunity [J]. Cell reports Medicine, 2022, 3(9).100744.
34. Wang S, Wu Z Z, Zhu S W, et al. CTLA-4 blockade induces tumor pyroptosis via CD8(+) T cells in head and neck squamous cell carcin

oma [J]. Molecular therapy : the journal of the American Society of Gene Therapy, 2023, 31 (7).2154-68.
35. Marquard F E, Jücker M. PI3K/AKT/mTOR si gnaling as a molecular target in head and neck cancer [J]. Biochemical pharmacology, 2020, 172113729.
36. Marques A E M, Borges G A, Viesi Do Nasci mento Filho C H, et al. Expression profile of t he PI3K-AKT-mTOR pathway in head and ne ck squamous cell carcinoma: Data from Brazil ian population [J]. Oral surgery, oral medicine, oral pathology and oral radiology, 2022, 133 (4).453-61.
37. Wang D, Jin X, Lei M, et al. USF1-ATRAP-P BX3 Axis Promote Breast Cancer Glycolysis a nd Malignant Phenotype by Activating AKT/ mTOR Signaling [J]. International journal of b iological sciences, 2022, 18(6).2452-71.
38. Su Y C, Lee W C, Wang C C, et al. Targeting PI3K/AKT/mTOR Signaling Pathway as a Ra diosensitization in Head and Neck Squamous Cell Carcinomas [J]. International journal of molecular sciences, 2022, 23(24).
39. Jiang Q, Xiao J, Hsieh Y C, et al. The Role of the PI3K/Akt/mTOR Axis in Head and Neck S quamous Cell Carcinoma [J]. Biomedicines, 2 024, 12(7).
40. Mody M D, Rocco J W, Yom S S, et al. Head a nd neck cancer [J]. Lancet (London, England), 2021, 398(10318).2289-99.
41. Chakladar J, John D, Magesh S, et al. The Intr atumor Bacterial and Fungal Microbiome Is C haracterized by HPV, Smoking, and Alcohol C onsumption in Head and Neck Squamous Cell Carcinoma [J]. International journal of molecu lar sciences, 2022, 23(21).